Structure of the Lennard-Jones liquid estimated from a single simulation

Shibu Saw [*] and Jeppe C. Dyre [†]

"Glass and Time," IMFUFA, Department of Science and Environment, Roskilde University, P.O. Box 260, DK-4000 Roskilde, Denmark

(Received 22 September 2020; revised 7 December 2020; accepted 8 December 2020; published 12 January 2021)

Combining the recent Piskulich-Thompson approach [Z. A. Piskulich and W. H. Thompson, J. Chem. Phys. **152**, 011102 (2020)] with isomorph theory, from a single simulation the structure of a single-component Lennard-Jones (LJ) system is obtained at an arbitrary state point in almost the whole liquid region of the temperature-density phase diagram. The LJ system exhibits two temperature ranges where the van't Hoff assumption that energetic and entropic forces are temperature independent is valid to a good approximation. A method to evaluate the structure at an arbitrary state point along an isochore from the knowledge of structures at two temperatures on the isochore is also discussed. We argue that, in general, the structure of any hidden scale-invariant system obeying the van't Hoff assumption in the whole range of temperatures can be determined in the whole liquid region of the phase diagram from a single simulation.

DOI: 10.1103/PhysRevE.103.012110

I. INTRODUCTION

The structure of an equilibrium liquid is characterized by the radial distribution function $g(r)$. This quantity can be obtained by light scattering experiments, simulations, or liquid state theory [1–3]. The radial distribution function provides not only an idea of the structure, but also facilitates in predicting various thermodynamics quantities as $g(r)$ is related to the latter through interparticle interactions [4]. The static structure factor, which is the Fourier transform of $g(r)$, is an input of the mode-coupling theory (MCT), which yields dynamical quantities such as the mean-squared displacement (MSD) or the intermediate scattering function [5,6].

Experiments are tricky to perform for supercooled liquids, which may have a strong tendency to crystallize. Simulations are equally difficult and need to be performed for a very long time due to associated long relaxation times [7]. Theoretical study of the temperature dependence of the structure will facilitate the prediction of structure from limited experimental or simulation data; however, such studies are limited [8]. Piskulich and Thomson [9] have recently shown that the radial distribution function $g(r)$ of TIP4P/2005 water [10] at several temperatures can be obtained from a single simulation. This theory is based on the van't Hoff assumption [11] that the energetic and entropic forces are temperature independent.

In this paper, we test the van't Hoff assumption for the single-component Lennard-Jones (LJ) system. This assumption is not valid for the whole range of temperatures, but it is approximately valid for two ranges of temperatures separately. The Piskulich-Thompson theory, then, is employed to the LJ system to predict the structure at other temperatures along the same isochore in each temperature range separately. We also prescribe a method to predict the structure from knowledge of $g(r)$ at two different temperatures along the same isochore, without performing any simulation or experiment.

A class of systems exhibits a strong correlation between virial and potential-energy equilibrium fluctuations, such as the inverse power law, LJ, etc., are known as a Roskilde or R-simple system. Along an isomorph [12–15], an R-simple system's structure and dynamics are invariant in reduced units [16,17]. We combine here the Piskulich-Thompson [9] approach with isomorph theory to predict the structure of the LJ system at an arbitrary state point in the liquid region of the temperature-density phase diagram.

We describe the Piskulich-Thompson theory in Sec. II. Section III describes the simulation method used. The results are given in Sec. IV. Section V explains how $g(r)$ along an isochore can be obtained without any simulation if the radial distribution functions at two temperatures along the same isochore are known. The extension of the Piskulich-Thompson theory for R-simple liquids is described in Sec. VI. A discussion and a summary are given in Sec. VII.

II. PISKULICH-THOMPSON THEORY

The radial distribution function is defined by [18]

$$g(r) = \frac{V}{N^2}\left\langle \sum_i \sum_{j\neq i} \delta(r - r_{ij}) \right\rangle, \tag{1}$$

where r_{ij} is the distance between particles i and j, and V and N are the volume and the number of particles, respectively. The $\langle \cdots \rangle$ represents an ensemble average. Since $\sum_i \sum_{j\neq i} \delta(r - r_{ij})$ does not depend on the momenta, Eq. (1) can be rewritten as

$$g(r) = \frac{V}{N^2}\frac{1}{Z}\int d\mathbf{q} e^{-\beta \mathcal{U}} \sum_i \sum_{j\neq i} \delta(r - r_{ij}), \tag{2}$$

[*] shibus@ruc.dk
[†] dyre@ruc.dk

in which $d\mathbf{q}$ are the system coordinates and $\beta = (k_B T)^{-1}$, where k_B and T are the Boltzmann constant and temperature, respectively. Z and $\mathcal{U}$ are the configurational canonical partition function and potential energy of the system. The temperature dependence of the radial distribution function $g(r)$ is given by [9]

$$\frac{\partial g(r)}{\partial \beta} = -\frac{V}{N^2}\left\langle \Delta\mathcal{U} \sum_i \sum_{j\neq i} \delta(r - r_{ij}) \right\rangle, \tag{3}$$

where $\Delta\mathcal{U} = \mathcal{U} - \langle \mathcal{U} \rangle$ is the fluctuation of potential energy from its mean value $\langle U \rangle$ (note that U is the total potential energy of a configuration, not of an individual particle).

The Helmholtz free energy profile $A(r)$ can be written in terms of the radial distribution function $g(r)$ as [9]

$$A(r) = -k_B T \ln g(r) - k_B T \ln v(r), \tag{4}$$

where $v(r) = r^2$ is a geometric factor. Without the geometric factor, the free energy is simply the potential of mean force $F_{PM}(r)$. The derivative of the Helmholtz free energy with respect to β is given by

$$\frac{\partial A(r)}{\partial \beta} = k_B T \left[\frac{g_H(r)}{g(r)} + k_B T \ln g(r) + k_B T \ln v(r) \right] \tag{5}$$

$$= k_B T \left[\frac{g_H(r)}{g(r)} - A(r) \right], \tag{6}$$

where $g_H(r) \equiv -\frac{\partial g(r)}{\partial \beta}$. The Helmholtz free energy $A(r)$ can be written in terms of internal energy and entropy as

$$A(r) = U(r) - TS(r). \tag{7}$$

With the assumption that $U(r)$ and $S(r)$ do not depend on the temperature (van't Hoff assumption), a comparison of Eqs. (6) and (7) yields expressions for the internal energy and the entropy as

$$U(r) = \frac{g_H(r)}{g(r)} \tag{8}$$

and

$$S(r) = \frac{1}{k_B T^2} \frac{\partial A(r)}{\partial \beta}. \tag{9}$$

$U(r)$ can be readily evaluated from Eqs. (1) and (3), and the entropy $S(r)$ can be determined from Eqs. (5), (3), and (1). Thus one can calculate the value of $U(r)$ and $S(r)$ from simulation data at a reference temperature T_0. Now from Eq. (4), the radial distribution function at an arbitrary temperature T, but same density, can be written as

$$g(r;\beta) = \frac{1}{v(r)} e^{-\beta U(r)} e^{S(r)/k_B}, \tag{10}$$

where $U(r)$ and $S(r)$ are evaluated at T_0. The above equation gives rise to the van't Hoff plot [19] if $U(r)$ and $S(r)$ are assumed to be temperature independent.

Substituting the values of $U(r)$ from Eq. (8) and $\frac{\partial A(r)}{\partial \beta}$ from Eq. (5), Eq. (10) becomes [9]

$$g(r;\beta) = g(r;\beta_0) e^{U(r)(\beta_0 - \beta)}. \tag{11}$$

This expression of $g(r;\beta)$ depends only on $U(r) \equiv \frac{g_H(r)}{g(r)}$. It is emphasized again that in the derivation, the van't Hoff assumption is assumed.

III. SIMULATION DETAILS

We have performed a canonical ensemble molecular dynamics simulation (NVT) of the LJ system employing a Nose-Hover thermostat with $N = 2000$ particles at various densities and temperatures. Employing a shifted-forces cutoff [20], the LJ interaction potential between particle i and j is given as

$$\frac{\phi(r_{ij})}{4\epsilon} = \begin{cases} \left(\frac{\sigma}{r_{ij}}\right)^{12} - \left(\frac{\sigma}{r_{ij}}\right)^{6} + C_1 r + C_2, & r_{ij} < 2.5\sigma \\ 0, & r_{ij} \geqslant 2.5\sigma, \end{cases} \tag{12}$$

where C_1 and C_2 ensure that the $\phi(r)$ and its first derivative are continuous at the cutoff, $r = 2.5\sigma$. The simulations were performed using RUMD (Roskilde University Molecular Dynamics) software [21], which is a graphical processing unit (GPU) code. Unless otherwise stated, all quantities reported in this paper are in LJ units: length, time, and temperature are expressed in units of σ, $\sqrt{m\sigma^2/\epsilon}$, and ϵ/k_B, respectively. We have used the state-point dependent molecular dynamics (MD) time step given by $\Delta t = 0.001\sqrt{m/(k_B T \rho^{2/3})}$. Most of the data result from 5×10^7 steps equilibration followed by 2×10^8 steps production run.

IV. RESULTS

A. The validity of the van't Hoff assumption

If the van't Hoff assumption is correct, then from Eq. (10) or Eq. (11) $\ln g(r;\beta)$ vs β should be a straight line. We plot the $g(r)$ against $1/T$ in log-linear scale in Fig. 1(a) for the LJ system at density $\rho = 0.80$ for a range of r values. It shows that the $\ln g(r)$ vs $1/T$ are not straight lines throughout the considered temperature range. This means that the van't Hoff assumption that $U(r)$ and $S(r)$ are temperature independent is not generally correct. The van't Hoff assumption has been seen not to be valid in other liquids or liquid mixtures with covalent bonds [22,23], as well. Interestingly, the van't Hoff assumption is not valid for the LJ system, which is a very simple liquid without any covalent bonds. However, two temperature ranges can be assigned where $\ln g(r)$ vs $1/T$ plots are fairly straight lines (though with different slopes). The main variation of $g(r)$ with inverse temperature is seen near the first peak of $g(r)$, i.e., near $r = 1.0$. Figure 1(b) exhibits the $1/T$ dependence of $g(r)$ at $r = 1.0$. It shows a nonmonotonic behavior with a maximum near $T = 3.0$. On either side of the peak the plot is an approximately straight line, and thus the van't Hoff assumption holds good in two temperature ranges, one at low T and another at high T.

In passing we note that this peak position should not be taken to be an isosbestic point. Isosbestic points have been observed in the oxygen-oxygen radial distribution function $g_{OO}(r)$ in water [24–26] where $\partial g(r)/\partial\beta = 0$. In the present case $\partial g(r)/\partial\beta$ at $r = 1.0$ is zero due to the presence of a peak unlike isosbestic points which are temperature independent. The first isosbestic point for the LJ system at density $\rho = 0.80$ is 1.33 (not shown).

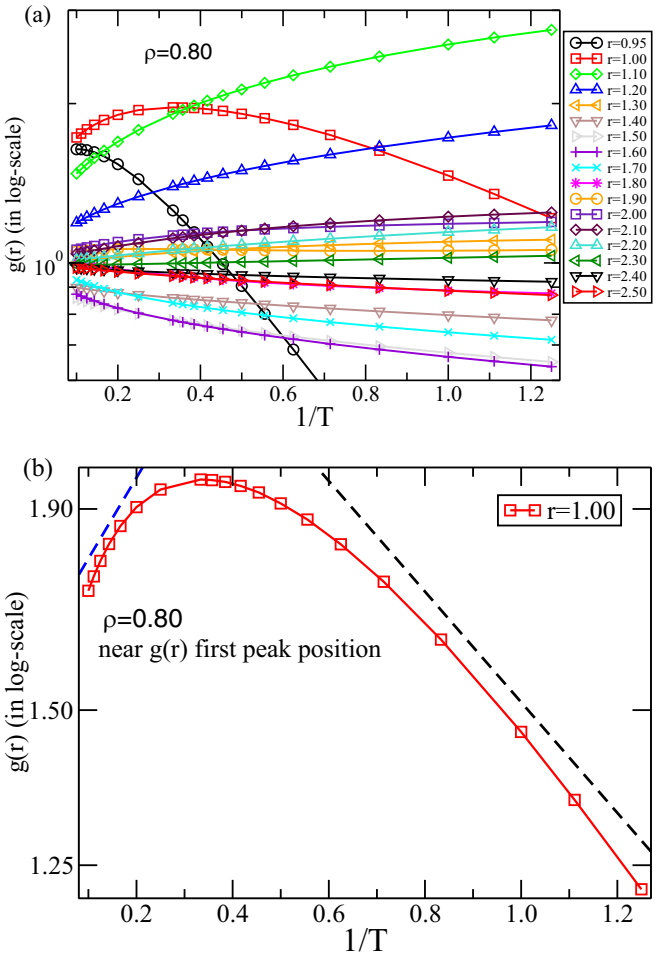

FIG. 1. T^{-1} dependence of $g(r)$ of a LJ system at density $\rho = 0.80$ in log-linear scale for (a) different values of r and (b) $r = 1.0$. The dashed lines are guides to the eye.

B. Application of Piskulich-Thompson theory

We now apply the Piskulich-Thompson theory at two temperatures, one on each side of the peak in Fig. 1(b) where the van't Hoff assumption is approximately valid, in order to determine $g(r)$ at other temperatures on that side. Figure 2(a) exhibits $g(r)$ at $T = 0.80$, 1.00, 1.20, 2.20, 2.60, and 3.00 obtained by applying Piskulich-Thompson theory at reference temperature $T_0 = 1.8$ and density $\rho = 0.80$. The radial distribution functions determined by employing Piskulich-Thompson theory (lines) have been compared with those obtained from MD simulation (symbols). They are in good agreement. The data have been shifted upward for clarity. Figure 2(b) shows the comparison of $g(r)$ at $T = 3.0$, 4.0, 5.0, 7.0, 8.0, and 10.0 determined from Piskulich-Thompson theory applied at $T_0 = 6.0$ (lines) with that obtained from direct MD simulations (symbols). The good agreement of the two $g(r)$ illustrates the following points: (i) the van't Hoff assumption is approximately valid in two separate temperature ranges at each side of the $g(r = 1.0)$ peak in Fig. 1(b) and (ii) the Piskulich-Thompson theory works for the LJ system in two temperature ranges.

Figure 2(c) shows the comparison between theoretical and simulation $g(r)$ at temperatures $T = 4.0$, 5.0, 6.0, 7.0, 8.0, and 10.0, which are on the high-temperature side of the peak in Fig. 1(b). The Piskulich-Thompson theory has been applied at $T_0 = 1.8$, which is on the low-temperature side of the peak in Fig. 1(b). With the increase of temperature, $g(r)$ obtained from theory deviates from the simulation one. A comparison of $g(r)$ for temperatures on the low-temperature side of the peak in Fig. 1(b) is shown in Fig. 2(d), where the theory has been applied at $T_0 = 6.0$, which is on the high-temperature side of the peak in Fig. 1(b). The two $g(r)$ again show disagreement, which worsens with the temperature moving away from $T = 3.0$, where $g(r)$ vs $1/T$ shows a peak. When the theory is applied at the peak position ($T = 3.0$), the disagreement between theoretical and simulation $g(r)$ is seen on both sides of the $g(r)$ vs $1/T$ peak (see Appendix A).

Figure 3 shows the van't Hoff demarcation line in the temperature-density phase diagram of the LJ system. The van't Hoff demarcation line has been estimated from the peak positions of $g(r)$ vs $1/T$ for different isochores (see Appendix B). The $g(r)$ vs $1/T$ shows a peak for several values of r. We have considered r satisfying $\rho^{1/3} r = 0.8^{1/3}$ in order to be close to the first peak position of the radial distribution function. The van't Hoff demarcation line increases with density. Figure 3 shows the melting line [27], freezing line [27], and liquid-vapor coexistence curve [28]. The two isomorphs also shown are discussed in Sec. VI. Though the van't Hoff demarcation line is well above the critical temperature, it is still much lower than the Frenkel line [29]. At density $\rho = 0.80$, temperatures of the Frenkel and van't Hoff demarcation lines are around $T = 14.0$ [29] and $T = 3.0$, respectively.

V. THE STRUCTURE AT AN ARBITRARY TEMPERATURE ALONG AN ISOCHORE ESTIMATED FROM TWO RADIAL DISTRIBUTION FUNCTIONS

Equation (11) can be rewritten as

$$U(r) = \frac{k_B T_0 T}{T - T_0} \ln\left[\frac{g(r;\beta)}{g(r;\beta_0)}\right], \tag{13}$$

where $\beta_0 = \frac{1}{k_B T_0}$. It is easy to show that the first-order Taylor expansion of $g(r;\beta)$ around $g(r;\beta_0)$ reduces Eq. (13) to Eq. (8) in the limit of $T \to T_0$. Thus $U(r)$ can be evaluated from $g(r)$ at two different temperatures at a given density. The procedure for obtaining $g(r)$, whether in experiments or simulations, is irrelevant. These two temperatures can be anywhere on the isochore in question, as long as the van't Hoff assumption is valid. However, one has no prior knowledge of the temperature range where the van't Hoff assumption is valid for the system under consideration. It is, therefore, intuitive to consider two temperatures that are not far away from each other, ensuring that the van't Hoff assumption is valid at least in that small temperature range. Once the $U(r)$ is determined, the $g(r)$ of liquids can be calculated at any temperature along the isochore from Eq. (11) without performing further simulation (or conducting more experiments). This is quite useful for a liquid with unknown interparticle interaction, and hence in this sense, the method is superior to standard liquid state theory, which requires the knowledge of the interactions between the particles.

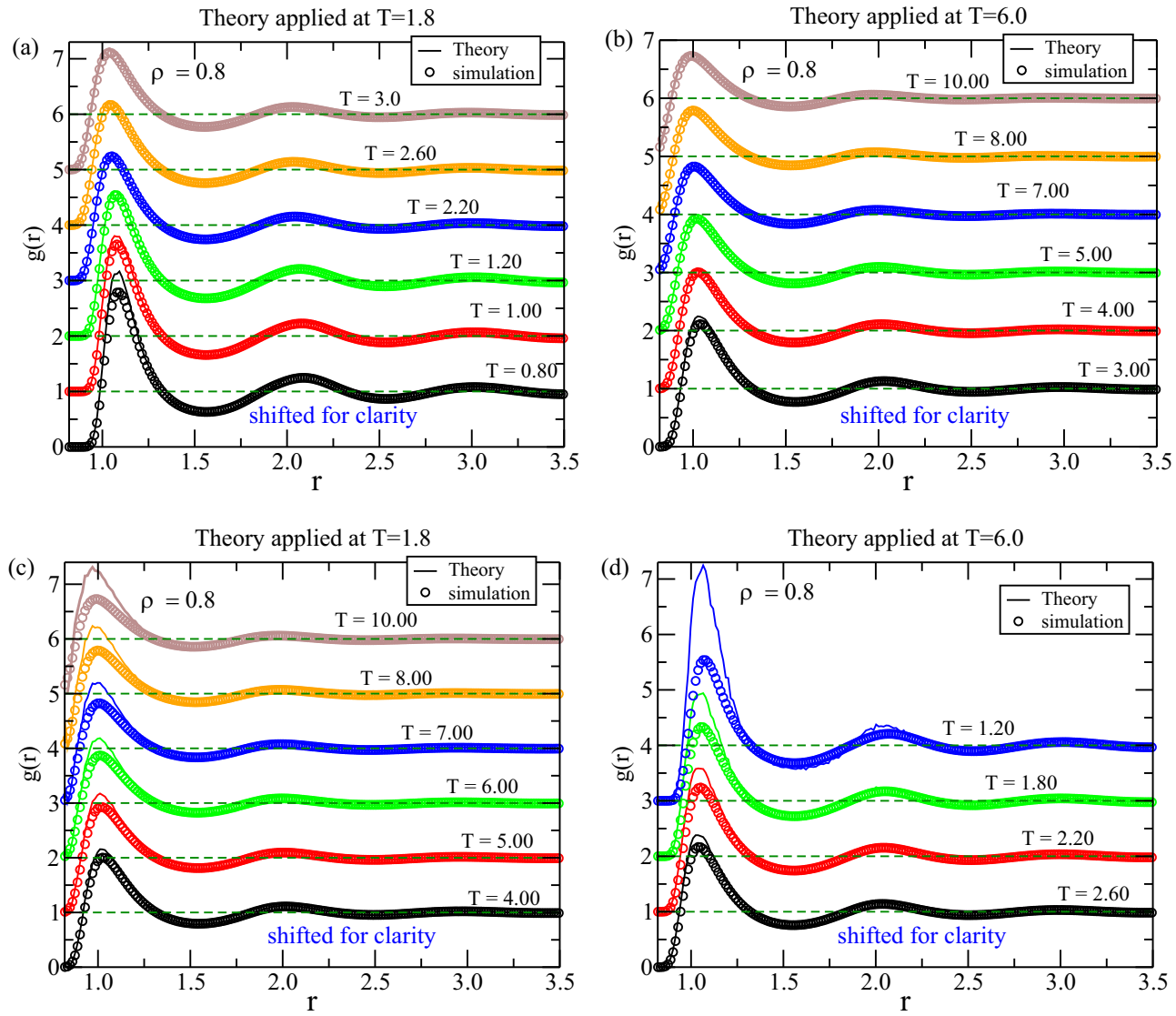

FIG. 2. A comparison of $g(r)$ estimated at various temperatures T by employing the Piskulich-Thompson theory at a reference temperature T_0 with that from simulations. (a) Both $T_0 = 1.8$ and various temperatures T are on the low-temperature side of the peak of $g(r = 1.0)$ vs $1/T$ in Fig. 1(b). (b) Both $T_0 = 6.0$ and various temperatures T are on the high-temperature side of the peak. (c) $T_0 = 1.8$ and various temperatures T are on the low- and high-temperature sides of the peak, respectively. (d) $T_0 = 6.0$ and various temperatures T are on the high- and low-temperature sides of the peak, respectively. The density is $\rho = 0.80$.

Figure 4(a) shows the comparison of $U(r)$ obtained by using Eqs. (13) and (8) at $T = 30$, $T = 45$, and $T = 80$ at density $\rho = 2.0$. The $U(r)$ at $T = 30$ has been evaluated using $g(r)$ at temperatures $T = 30$ and $T = 32$. Similarly, the function $U(r)$ at $T = 45$ and $T = 80$ has been obtained from $g(r)$ at $T = 45$ and $T = 50$ and at $T = 80$ and $T = 75$, respectively. The $U(r)$ at these three temperatures obtained by using Eq. (13) (lines) is in good agreement with that obtained from MD simulations (symbols) directly. In MD simulations Eq. (8) is employed to evaluate $U(r)$. Thus, unlike the Piskulich-Thompson theory, one does not need the fluctuation of potential energy $\Delta\mathcal{U}$ to evaluate $U(r)$. Figure 4(b) shows a comparison of $g(r)$ obtained from $U(r)$ evaluated by employing Eq. (13) ($T_0 = 45$, $T = 50$) with the one determined by employing the Piskulich-Thompson theory at $T_0 = 45$ (symbols) at temperatures $T = 30$, 45, and 80. They are in good agreement with one another. Filled symbols for the temperature $T = 30$ indicate that the liquid is supercooled. The theory works alike for normal and supercooled liquids. As mentioned, this method opens up the possibility of predicting the $g(r)$ along an isochore of a liquid for which the interparticle interactions are unknown if its $g(r)$ at two nearby temperatures are available, say, from light scattering experiments. This method is robust for the temperature range where the van't Hoff assumption is valid.

VI. PISKULICH-THOMPSON + ISOMORPH THEORY

So far we have discussed the determination of $g(r)$ along an isochore either (i) directly using Piskulich-Thompson theory or (ii) by employing Eqs. (11) and (13) where only $g(r)$ at two temperatures is needed. Now we generalize this into a method

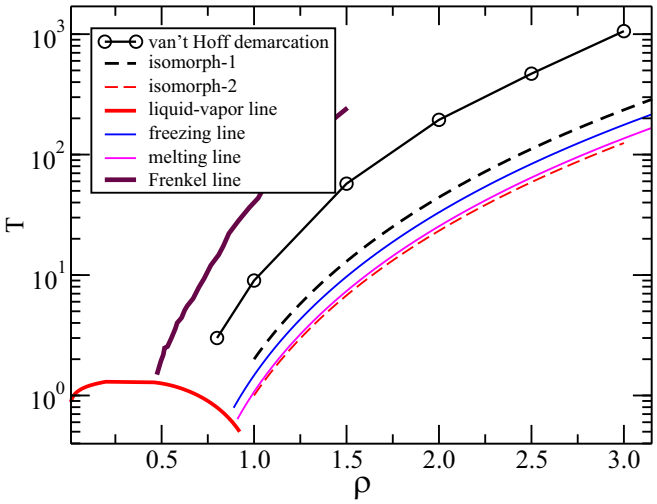

FIG. 3. The van't Hoff demarcation line, obtained from the peak positions of $g(r = (0.80/\rho)^{1/3})$ vs $1/T$ for various isochores, has been shown in the LJ phase diagram. The freezing line [27], melting line [27], liquid-vapor coexistence curve [28], and Frenkel line [29] are also shown.

to calculate $g(r)$ at an arbitrary temperature in the T-ρ phase diagram from just one simulation at the reference state point (ρ_0, T_0). To achieve this we combine the Piskulich-Thompson theory with isomorph theory. First we determine the isomorph passing through the reference point (ρ_0, T_0). The equation for an isomorph of the LJ system is given by [30–32]

$$\frac{T(\rho)}{T_0} = \left(\frac{\gamma_0}{2} - 1\right)\left(\frac{\rho}{\rho_0}\right)^4 - \left(\frac{\gamma_0}{2} - 2\right)\left(\frac{\rho}{\rho_0}\right)^2, \quad (14)$$

where the so-called density-scaling exponent γ_0 is calculated from the equilibrium constant-volume fluctuations at the reference state point by means of

$$\gamma_0 = \frac{\langle \Delta\mathcal{U}\Delta W\rangle}{\langle(\Delta\mathcal{U})^2\rangle}. \quad (15)$$

Here, $\Delta\mathcal{U}$ and ΔW are fluctuations in potential energy and virial.

Figure 5(a) exhibits $g(r)$ at various state points along the isomorph starting from the reference state point $(\rho_0, T_0) = (1, 2)$ for the LJ system. The inset of Fig. 5(b) shows the isomorph (line) and the state points (red symbols) where MD simulations have been performed. This isomorph is shown in Fig. 3 as isomorph-1, which is above the freezing line. The main panel of Fig. 5(b) shows the $g(r)$ in Fig. 5(a) in isomorph-reduced units. The color scheme for both main panels is the same.

As expected, $g(r)$ is invariant in isomorph-reduced units; i.e., $g(\rho^{1/3}r) = \text{const}$ along the isomorph [Fig. 5(b)]. Hence, the $g(r)$ of the system at any point of the isomorph, say, (ρ_1, T_1), can be obtained easily from the $g(r)$ of the reference point (ρ_0, T_0). Thereafter, the Piskulich-Thompson theory can be employed along the isochore at ρ_1. In order to apply the Piskulich-Thompson theory we require the potential energy at (ρ_1, T_1), which is different from that at the reference state point (ρ_0, T_0). Fortunately, the potential energy at (ρ_1, T_1)

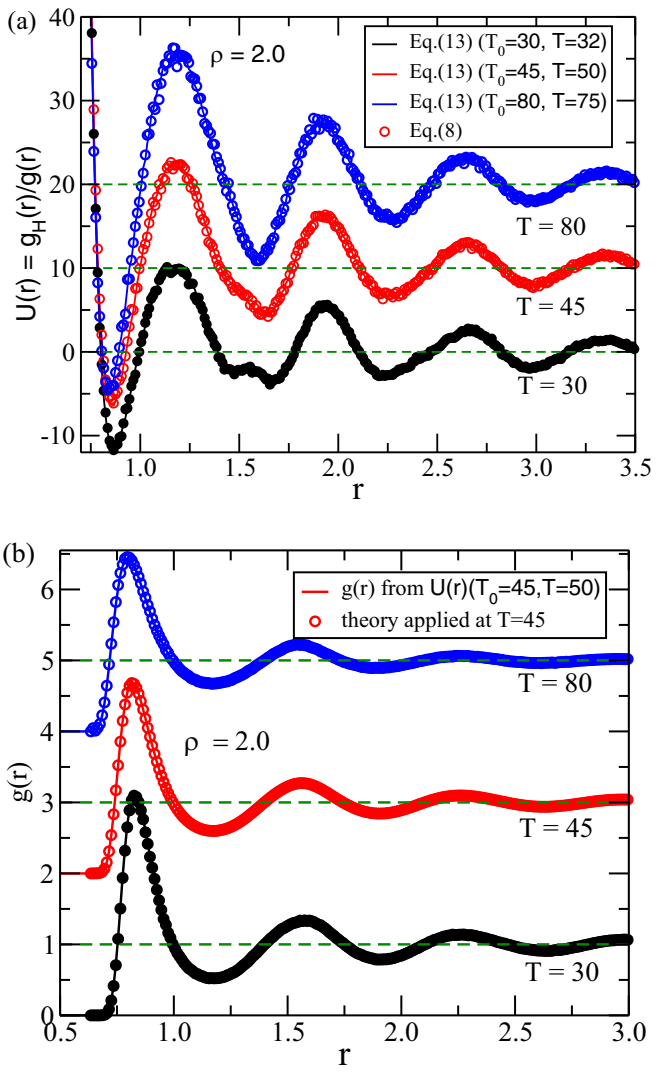

FIG. 4. (a) The comparison of $U(r)$ for the LJ system at density $\rho = 2.0$ and $T = 30$, $T = 45$, and $T = 80$ obtained from fitting to Eqs. (13) and (8). The data have been shifted upward for clarity by 10 units. (b) Comparison of $g(r)$ obtained from Piskulich-Thompson theory with that obtained from $U(r)$ using Eq. (13) instead of from simulation data. The data have been shifted upward by 2 units for clarity.

can also be obtained by scaling the potential energy at the reference point (ρ_0, T_0) by proceeding as follows. The scaled potential energy $\mathcal{U}$ of the LJ system at (ρ_1, T_1) in terms of potential energy at the reference point (ρ_0, T_0) is given by [33]

$$\mathcal{U} = \tilde{\rho}^{m/3}\mathcal{U}_0^m + \tilde{\rho}^{n/3}\mathcal{U}_0^n, \quad (16)$$

where $\tilde{\rho} = \rho_1/\rho_0$ and $\mathcal{U}^k$ is the potential-energy contribution from the r^{-k} term of the LJ pair potential. The $\mathcal{U}^m$ and $\mathcal{U}^n$ are the repulsive and attractive parts of the LJ potential (and hence $m = 12$ and $n = 6$), respectively, implying that

$$\mathcal{U} = \mathcal{U}^m + \mathcal{U}^n, \quad (17)$$

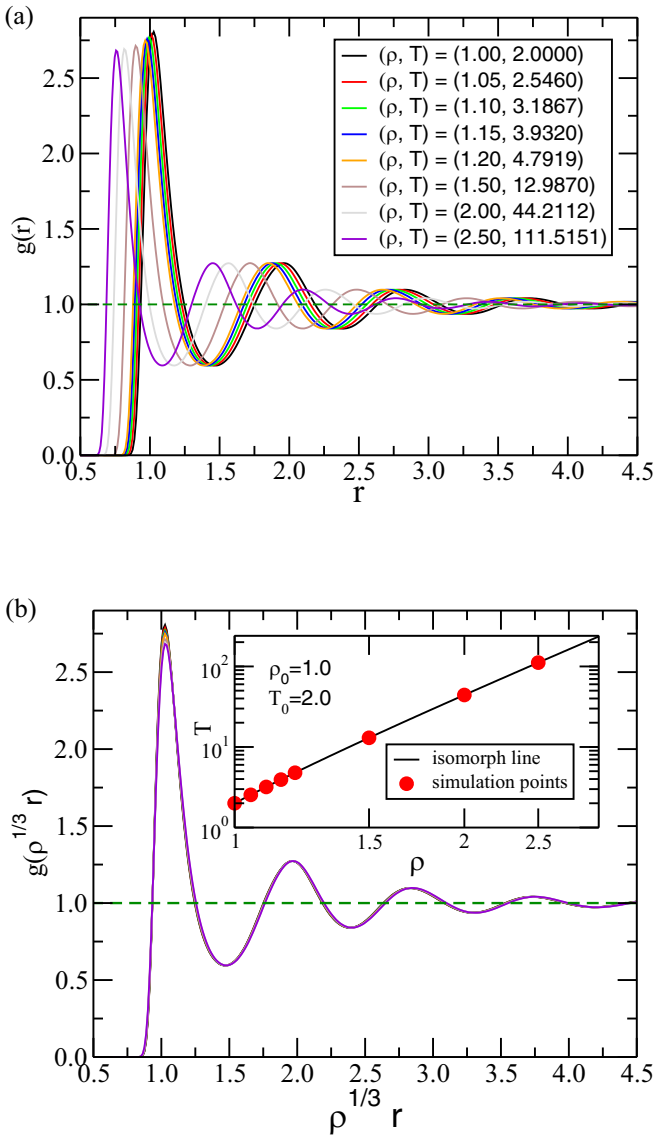

FIG. 5. (a) $g(r)$ at different state points on the isomorph; (b) same $g(r)$ in isomorph-reduced units. The color scheme for both main panels is the same. Inset: State points for which $g(r)$ is shown here.

in which $\mathcal{U}_0^m$ and $\mathcal{U}_0^n$ are the values of $\mathcal{U}^m$ and $\mathcal{U}^n$ at the reference point (ρ_0, T_0) on the isomorph. The $\mathcal{U}^m$ and $\mathcal{U}^n$ are given by [33]

$$\mathcal{U}^m = \frac{3W - m\mathcal{U}}{m-n}, \tag{18}$$

$$\mathcal{U}^n = \frac{-3W + m\mathcal{U}}{m-n}. \tag{19}$$

The above equation is based on the fact that $\frac{\mathcal{U}^k}{\rho^{k/3}} = \text{const}$ [ignoring the linear term in the shifted-force cutoff LJ potential; see Eq. (12)].

Figure 6 shows a comparison of $-g_H(r)$ obtained from isomorph scaling and direct simulation at state points ($\rho = 1.2$, $T = 4.79$), ($\rho = 1.5, T = 12.98$), ($\rho = 2, T = 44.21$), and ($\rho = 2.5, T = 111.51$) on the isomorph. The $-g_H(r)$ obtained from isomorph scaling (lines) described above are in

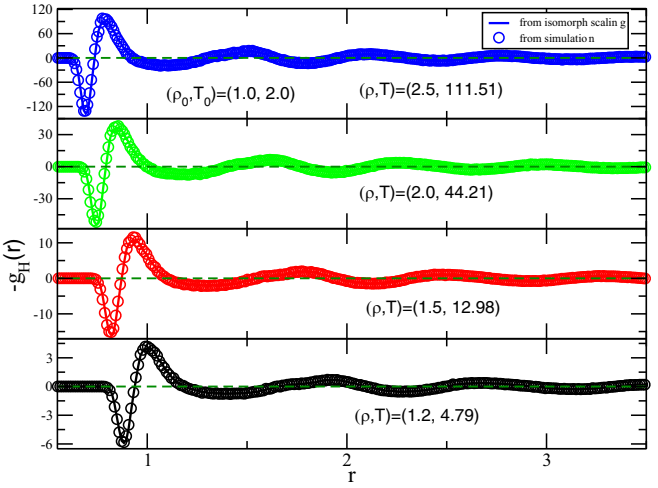

FIG. 6. The comparison of $-g_H(r)$ obtained from isomorph scaling and direct simulation at different points on the isomorph.

good agreement with those obtained from MD simulations (open symbols) at these state points.

Now we have $g(r)$ as well as $-g_H(r)$ [so $U(r)$] at the state point (ρ_1, T_1), and therefore, the Piskulich-Thompson theory can be applied easily. Figures 7(a)–7(d) show comparisons of $g(r)$ obtained by employing Piskulich-Thompson + isomorph theory with those from simulations. They are in good agreement when $|T - T_1|$ is small. The slight discrepancy at large $|T - T_1|$ is associated with the following two facts: (i) the LJ system obeys the van't Hoff assumption to a good approximation only in a limited temperature range and (ii) the isomorph theory is not good at capturing the first peak correctly [16]. One can observe the discrepancy between isomorph theory and simulation in $-g_H(r)$ near the first peak in Fig. 6, as well. To summarize, for a van't Hoff valid liquid, $g(r)$ can be calculated at any arbitrary state point in the liquid region of the temperature-density phase diagram from a single state point simulation.

VII. DISCUSSION AND SUMMARY

The van't Hoff assumption is that the energetic and entropic forces are temperature independent. We have shown that the LJ system disobeys the van't Hoff assumption when viewed over the entire temperature range studied. Unlike other non–van't Hoff liquids [22,23], the LJ system does not have any covalent bond. The fact that the van't Hoff assumption breaks down might be due to a different activation energy at low and high temperatures. At very high temperature, the LJ system is governed by entropic forces and energy plays little role, but at low temperature the energy dominates and some of the particles remain close to one another for quite a long time, behaving as a quasicovalent bond.

While the van't Hoff assumption for the LJ system is not valid for the whole range of temperatures studied, there are two distinct temperature ranges [see Fig. 1(b)] where the van't Hoff assumption applies approximately. This is validated by the excellent agreement of the $g(r)$ obtained from Piskulich-Thompson theory and simulation [see Figs. 2(a) and

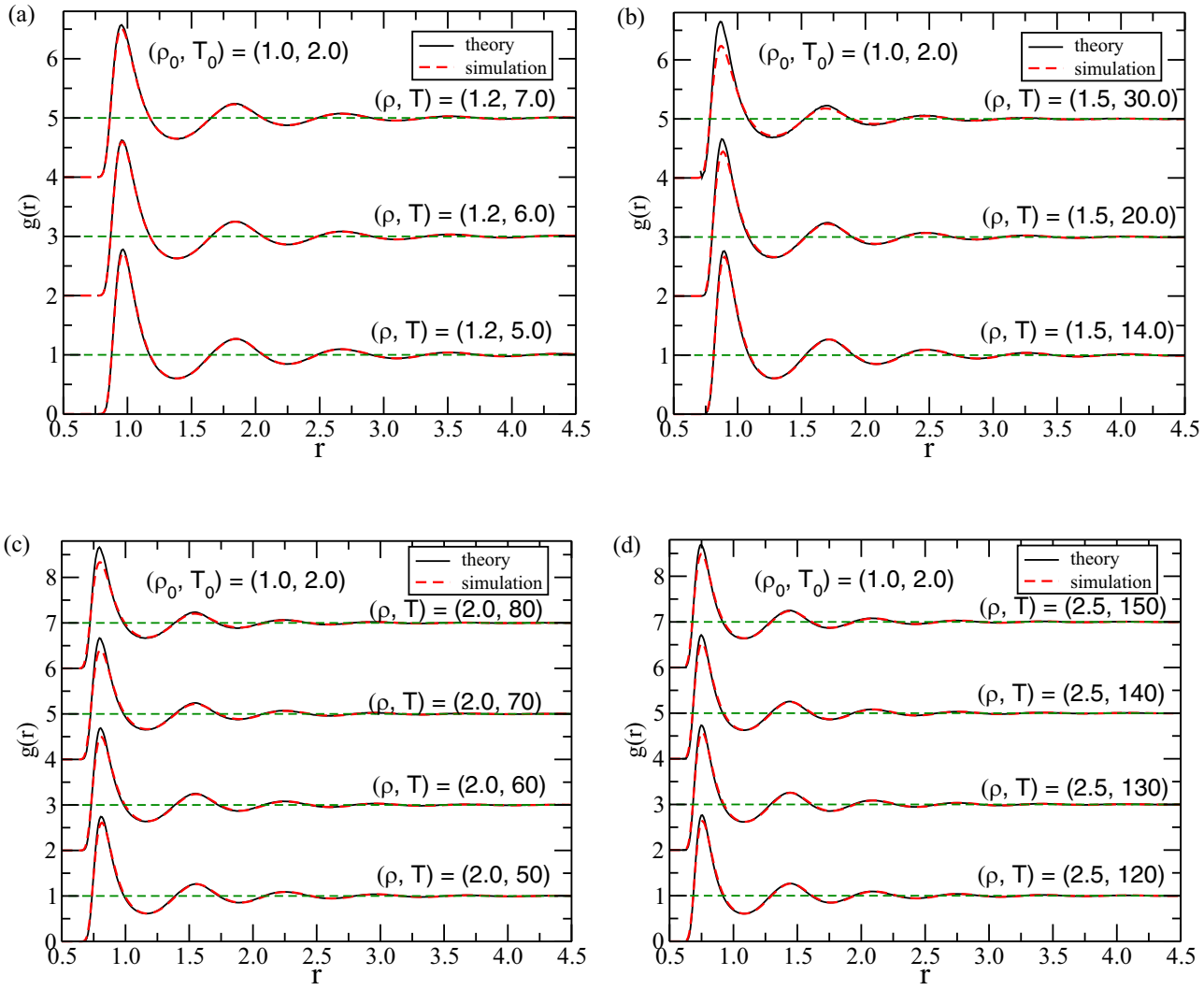

FIG. 7. The comparison of $g(r)$ obtained by employing Piskulich-Thompson + isomorph theory with that from simulation at different state points of an isochore: (a) $\rho = 1.20$, (b) $\rho = 1.50$, (c) $\rho = 2.00$, and (d) $\rho = 2.50$. The reference temperature and density for Piskulich-Thompson + isomorph theory is ($\rho_0 = 1.0$, $T_0 = 2.0$). The data have been shifted upward by 2 units for clarity.

2(b)]. The Piskulich-Thompson theory has been applied at one temperature in each low-T range ($T = 1.8$) and high-T range ($T = 6$) to determine $g(r)$ at other temperatures in that range [see Figs. 2(a) and 2(b)]. For a van't Hoffian system, a single simulation is enough to determine $g(r)$ at an arbitrary temperature at the same density employing Piskulich-Thompson theory. For a non–van't Hoffian system, such as the LJ, the range of temperatures where Piskulich-Thompson theory can be applied to determine $g(r)$, is limited. Thus for such a system, one can only determine $g(r)$ at the temperatures in the vicinity of the state point where simulation data are available.

Simulations of supercooled liquids are challenging due to their long relaxation time and strong crystallization tendency. At such low temperatures, the van't Hoff assumption would probably be valid for all systems, and thus Piskulich-Thompson theory can be applied. In such a scenario, this theory could be helpful. In Appendix C, we show that the theory indeed works equally well for supercooled liquids.

We have shown that the energetic force $U(r)$ can be evaluated from a knowledge of $g(r)$ at two temperatures, in the van't Hoff region [see Eq. (13)]. This method is particularly useful when the interatomic and/or intermolecular interactions are not known, forbidding computer simulations, or when simulations and/or experiments are extremely challenging. Since many systems may have multiple temperature ranges with a valid van't Hoff assumption similar to the LJ system, it is best to consider $g(r)$ at two close temperatures, where the van't Hoff assumption is bound to be valid. Once $U(r)$ is determined, $g(r)$ can be predicted at various temperatures along the isochore if the van't Hoff assumptions holds.

The Piskulich-Thompson theory works only along an isochore. We have extended this theory to calculate the $g(r)$ at an arbitrary state point of the liquid region of the phase diagram from a single simulation at a reference state point (ρ_0, T_0). For this, we have combined the Piskulich-Thompson approach with the isomorph theory. The structure of a liquid along an isomorph is invariant in isomorph-reduced units. It should be noted that not all systems have isomorphs (are R-simple) [34]—water is a striking counterexample—and the current approach is of course limited to R-simple liquids. The

isomorph theory is not valid in the gaseous region of the LJ system either [16,35], and hence this theory cannot be applied to determine the radial distribution function in the low-density region of the LJ phase diagram.

In order to calculate $g(r)$ at state point (ρ, T), we first calculate $g(r)$ at (ρ, T_{iso}), where T_{iso} is on the isomorph. We here need to scale the potential energy from the reference point to the (ρ, T_{iso}) as well. For the LJ system, this is done as shown in Eqs. (18) and (19) following Ref. [33]. This expression is system dependent, and one needs to find the expression for other potentials as per the isomorph theory described in Ref. [33]. Thus $U(r) = g_H(r)/g(r)$ is known at (ρ, T_{iso}). Thereafter, the Piskulich-Thompson theory is employed along the isochore ρ to calculate $g(r)$ at the designated state point (ρ, T).

Again, for a perfect van't Hoffian system, $g(r)$ at every state point of the phase diagram (liquid region) can be obtained. On the other hand, if the system does not have a single temperature range where the van't Hoff assumption is valid, this theory cannot be used to evaluate $g(r)$ in the whole liquid phase of the diagram from a single simulation. But if the information of different temperature ranges and data from one simulation in each temperature range are available, one can calculate $g(r)$ in the whole liquid phase part of the phase diagram for an R-simple system. We again remind that not all systems have isomorphs [13,34]. However, many systems are indeed R-simple [13] and Piskulich-Thompson + isomorph theory should apply to any such system.

All thermodynamic quantities are related to the radial distribution function $g(r)$, and hence they can be evaluated in the liquid region of the phase diagram whenever the above theory is applicable. But again, there are systems with three-body interactions such as silicon [36–38] where the theory will not be applicable. As far as dynamics is concerned, the MCT requires the structure factor [which is Fourier transform of $g(r)$] and the interparticle interactions to provide the dynamics such as MSD and the intermediate scattering function. Thus for an R-simple system, employing Piskulich-Thompson + isomorph theory along with MCT, one can calculate all thermodynamics as well as dynamical quantities.

In summary, we have shown the following:

(i) The LJ system generally disobeys the van't Hoff assumption that the energetic and entropic forces are temperature independent. However, one can identify two temperature ranges in which the van't Hoff assumption is valid to a good approximation. We validated this by comparing the $g(r)$ determined by employing Piskulich-Thompson theory with that obtained from the simulation, with excellent agreement.

(ii) One can obtain the energetic force term $U(r)$ without any simulation, and only $g(r)$ at two temperatures in the temperature range where the van't Hoff assumption is valid is required. Then $g(r)$ along an isochore can be calculated from $U(r)$ at all temperatures where the van't Hoff assumption is valid.

(iii) The $g(r)$ can be determined at an arbitrary state point in the liquid region of the phase diagram for an R-simple liquid from just a single simulation by employing Piskulich-Thompson + isomorph theory.

It would be interesting to investigate whether the van't Hoff assumption may be valid in the whole temperature range for other R-simple liquids, e.g., inverse-power law, Yukawa potential, or Morse potential systems.

ACKNOWLEDGMENT

This work was supported by the VILLUM Foundation's Matter grant (Grant No. 16515). We thank Lorenzo Costigliola for the fruitful discussions.

APPENDIX A: PISKULICH-THOMPSON THEORY APPLIED AT THE PEAK OF $\ln g(r = 1.0)$ VERSUS $1/T$

Piskulich-Thompson theory is applied at the reference temperature $T = 3.0$ for density $\rho = 0.80$ where $\ln g(r = 1.0)$ vs $1/T$ exhibits a peak [see Fig. 1(b)]. From Fig. 8 it is evident that the theory can predict the structure on either side of the peak only if the deviation from the reference temperature is small. Theory fails to estimate $g(r)$ on either side of the peak when deviations from the reference temperature are large.

APPENDIX B: VAN'T HOFF DEMARCATION LINE

Figure 9 exhibits the $1/T$ dependence of $g(r)$ for various isochores. We here consider r which satisfies $\rho^{1/3} r = 0.80^{1/3}$.

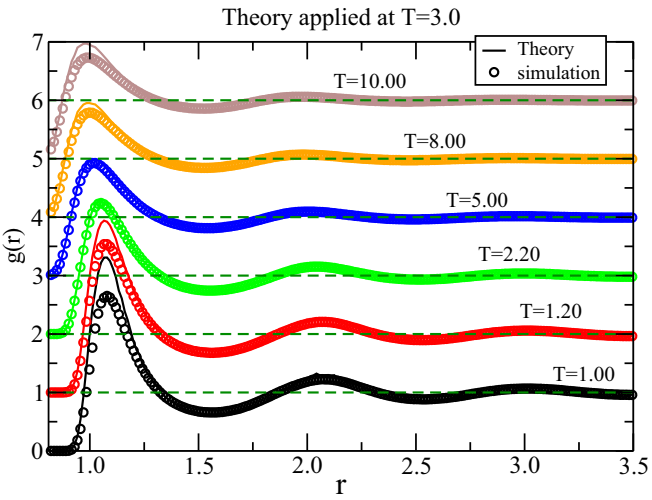

FIG. 8. A comparison of $g(r)$ obtained from simulations and by employing the Piskulich-Thompson theory at the peak in Fig. 1(b) ($T = 3.0$), at either side of the peak. The density is $\rho = 0.80$.

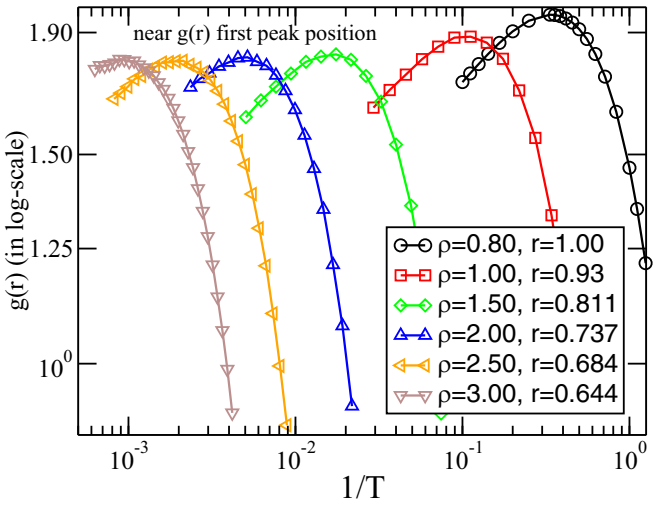

FIG. 9. T^{-1} dependence of $g(r)$ of the LJ system at various densities and r satisfying $\rho^{1/3}r = 0.80^{1/3}$.

The temperature, where $\ln g(r)$ vs $1/T$ shows a peak, increases with density. These temperatures construct the van't Hoff demarcation line (see Fig. 3). The van't Hoff assumption holds good on either side of the demarcation line in the phase diagram. One can determine the $g(r)$ at an arbitrary state point on either side of the van't Hoff demarcation line from a single simulation on the same side.

APPENDIX C: PISKULICH-THOMPSON + ISOMORPH THEORY APPLIED ALONG AN ISOMORPH IN THE SUPERCOOLED REGIME

In the main text, we have shown that Piskulich-Thompson + isomorph theory works well for normal LJ liquids. However, this theory works equally well in the supercooled regime of the LJ phase diagram. For supercooled liquids, the reference state point is $(\rho_0, T_0) = (1, 1)$; a supercooled isomorph is shown as "isomorph-2" in Fig. 3. Figure 10(a) shows the $g(r)$ at different state points along the isomorph in the supercooled regime, starting from the reference state point $(\rho_0, T_0) = (1, 1)$. The inset shows the state points where MD simulations are performed. Figure 10(b) shows that the $g(r)$ in the reduced units, i.e., $g(\rho^{1/3}r)$, is isomorph invariant.

Figure 11 is similar to Fig. 6, but for the isomorph in the supercooled regime. The $-g_H(r)$ obtained from isomorph scaling and simulations are in good agreement, similar to along the isomorph in the normal liquid regime (Fig. 6).

Figure 12 is similar to Fig. 7 except that the reference state point ($\rho_0 = 1, T_0 = 1$), where a single simulation is performed, is now in the supercooled regime. Figure 12 shows that Piskulich-Thompson + isomorph theory is able to determine the $g(r)$ at an arbitrary state point below the van't Hoff demarcation line.

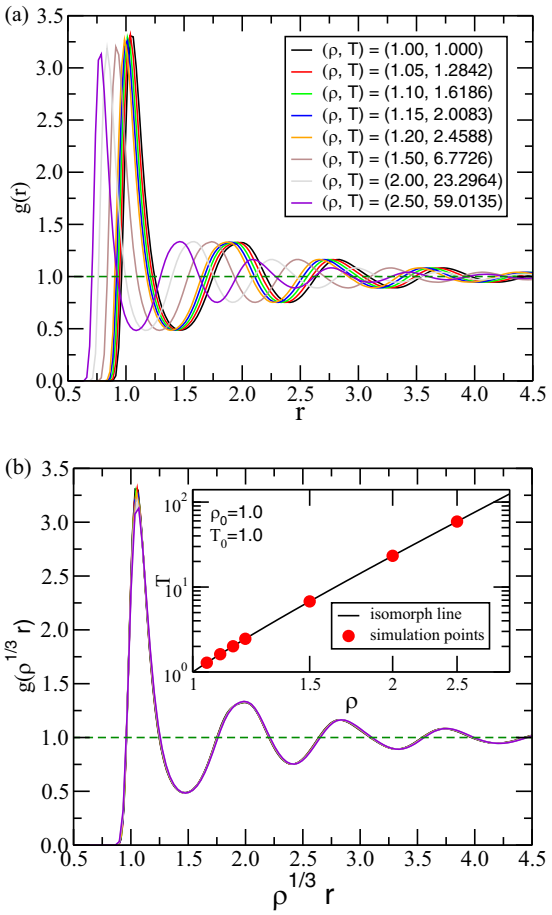

FIG. 10. (a) $g(r)$ at different state points on the isomorph starting from the reference state point $\rho_0 = 1.0$ and $T_0 = 1.0$ which is below the melting line; (b) same $g(r)$ in reduced units. The color scheme for both main panels is the same. Inset: Isomorph and state points for which $g(r)$ has been shown here.

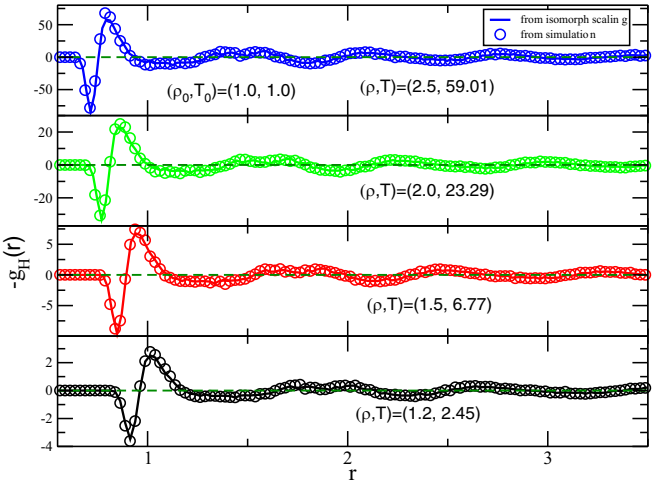

FIG. 11. A comparison of $-g_H(r)$ obtained from isomorph scaling and direct simulation at different state points on the supercooled isomorph (isomorph-2 in Fig. 3).

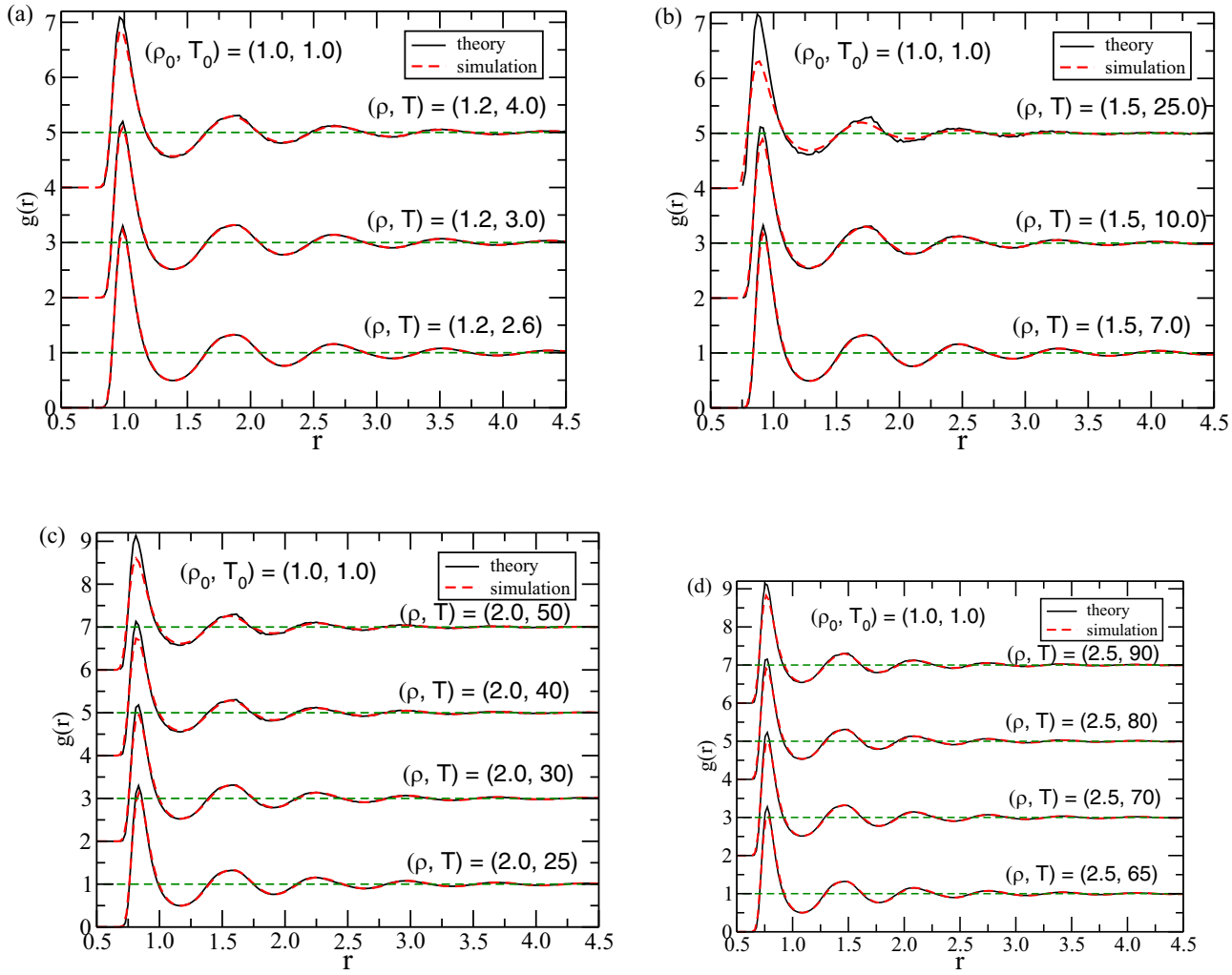

FIG. 12. A comparison of $g(r)$ obtained by employing Piskulich-Thompson + isomorph theory with that from simulation at different points of isochores: (a) $\rho = 1.20$, (b) $\rho = 1.50$, (c) $\rho = 2.00$, and (d) $\rho = 2.50$. The reference temperature and density for Piskulich-Thompson + isomorph theory is ($\rho_0 = 1.0$, $T_0 = 1.0$).

[1] J.-P. Hansen and I. R. McDonald, *Theory of Simple Liquids*, 3rd ed. (Elsevier, Boston, 2007).

[2] S. Saw, S. M. Kamil, and C. Dasgupta, Phys. Rev. E **91**, 052406 (2015).

[3] S. Chandran, S. Saw, A. K. Kandar, C. Dasgupta, M. Sprung, and J. K. Basu, J. Chem. Phys. **143**, 084902 (2015).

[4] D. McQuarrie, *Statistical Mechanics* (University Science Books, Sausalito, CA, 2000).

[5] W. Götze, J. Phys.: Condens. Matter **11**, A1 (1999).

[6] W. Kob, arXiv:cond-mat/0212344.

[7] L. Berthier and G. Biroli, Rev. Mod. Phys. **83**, 587 (2011).

[8] N. A. Mahynski, S. Jiao, H. W. Hatch, M. A. Blanco, and V. K. Shen, J. Chem. Phys. **148**, 194105 (2018).

[9] Z. A. Piskulich and W. H. Thompson, J. Chem. Phys. **152**, 011102 (2020).

[10] J. L. F. Abascal and C. Vega, J. Chem. Phys. **123**, 234505 (2005).

[11] D. Haidacher, A. Vailaya, and C. Horvath, Proc. Natl. Acad. Sci. USA **93**, 2290 (1996).

[12] T. S. Ingebrigtsen, T. B. Schrøder, and J. C. Dyre, Phys. Rev. X **2**, 011011 (2012).

[13] J. C. Dyre, J. Phys. Chem. B **118**, 10007 (2014).

[14] J. C. Dyre, J. Phys.: Condens. Matter **28**, 323001 (2016).

[15] J. C. Dyre, J. Chem. Phys. **149**, 210901 (2018).

[16] N. Gnan, T. B. Schrøder, U. R. Pedersen, N. P. Bailey, and J. C. Dyre, J. Chem. Phys. **131**, 234504 (2009).

[17] T. B. Schrøder and J. C. Dyre, J. Chem. Phys. **141**, 204502 (2014).

[18] M. P. Allen and D. J. Tildesley, *Computer Simulation of Liquids* (Oxford University Press, New York, 2017).

[19] P. Atkins and J. De Paula, *Physical Chemistry*, 8th ed. (Oxford University Press, New York, 2006).

[20] S. Toxvaerd and J. C. Dyre, J. Chem. Phys. **134**, 081102 (2011).

[21] N. P. Bailey, T. S. Ingebrigtsen, J. S. Hansen, A. A. Veldhorst, L. Bøhling, C. A. Lemarchand, A. E. Olsen, A. K. Bacher, L. Costigliola, U. R. Pedersen, H. Larsen, J. C. Dyre, and T. B. Schrøder, SciPost Phys. **3**, 038 (2017); http://rumd.org.

[22] J. G. Dorsey and W. T. Cooper, Anal. Chem. **66**, 857A (1994).

[23] T. Galaon and V. David, J. Sep. Sci. **34**, 1423 (2011).

[24] L. B. Skinner, C. J. Benmore, J. C. Neuefeind, and J. B. Parise, J. Chem. Phys. **141**, 214507 (2014).

[25] H. Pathak, A. Späh, K. H. Kim, I. Tsironi, D. Mariedahl, M. Blanco, S. Huotari, V. Honkimäki, and A. Nilsson, J. Chem. Phys. **150**, 224506 (2019).
[26] L. Bosio, S. H. Chen, and J. Teixeira, Phys. Rev. A **27**, 1468 (1983).
[27] L. Costigliola, T. B. Schrøder, and J. C. Dyre, Phys. Chem. Chem. Phys. **18**, 14678 (2016).
[28] D. M. Heyes, Comput. Methods Sci. Technol. **21**, 169 (2015).
[29] T. J. Yoon, M. Y. Ha, W. B. Lee, and Y.-W. Lee, J. Phys. Chem. Lett. **9**, 4550 (2018).
[30] T. S. Ingebrigtsen, L. Bøhling, T. B. Schrøder, and J. C. Dyre, J. Chem. Phys. **136**, 061102 (2012).
[31] L. Bøhling, T. S. Ingebrigtsen, A. Grzybowski, M. Paluch, J. C. Dyre, and T. B. Schrøder, New J. Phys. **14**, 113035 (2012).
[32] L. Costigliola, D. M. Heyes, T. B. Schrøder, and J. C. Dyre, J. Chem. Phys. **150**, 021101 (2019).
[33] T. B. Schrøder, N. Gnan, U. R. Pedersen, N. P. Bailey, and J. C. Dyre, J. Chem. Phys. **134**, 164505 (2011).
[34] N. P. Bailey, U. R. Pedersen, N. Gnan, T. B. Schrøder, and J. C. Dyre, J. Chem. Phys. **129**, 184507 (2008).
[35] A. Malins, J. Eggers, and C. P. Royall, J. Chem. Phys. **139**, 234505 (2013).
[36] F. H. Stillinger and T. A. Weber, Phys. Rev. B **31**, 5262 (1985).
[37] S. Saw, N. L. Ellegaard, W. Kob, and S. Sastry, Phys. Rev. Lett. **103**, 248305 (2009).
[38] S. Saw, N. L. Ellegaard, W. Kob, and S. Sastry, J. Chem. Phys. **134**, 164506 (2011).